

Supporting Information for

**Streamlined Approach to a New Gelator:  
Inspiration from Solid-State Interactions for a Mercury-induced Gelation**

Kelsey N. King and Anne J. McNeil\*

*Department of Chemistry and Macromolecular Science and Engineering Program  
University of Michigan, 930 North University Avenue, Ann Arbor, Michigan 48109-1055*

<b>Contents</b>	<b>Page</b>
<u>I. Materials</u>	S3
<u>II. General Experimental</u>	S3
<u>III. Synthetic Procedures</u>	
Synthesis of <b>2a</b>	S5
Synthesis of <b>2b</b>	S5
Synthesis of <b>2c</b>	S6
Synthesis of <b>S1</b>	S6
<u>IV. NMR Spectra</u>	
<b>Figure S1.</b> $^1\text{H}$ and $^{13}\text{C}$ NMR Spectra of <b>2a</b>	S7
<b>Figure S2.</b> $^1\text{H}$ and $^{13}\text{C}$ NMR Spectra of <b>2b</b>	S8
<b>Figure S3.</b> $^1\text{H}$ and $^{13}\text{C}$ NMR Spectra of <b>2c</b>	S9
<b>Figure S4.</b> $^1\text{H}$ and $^{13}\text{C}$ NMR Spectra of <b>S1</b>	S10
<u>V. Gelation Experiments</u>	
<b>Figure S5.</b> Gels of <b>2a</b> formed in situ and via isolated complex	S11
<b>Table S1.</b> Critical gel concentrations of <b>2a</b> (complex) in varying MeOH/H <sub>2</sub> O ratios	S11
<b>Table S2.</b> Critical gel concentrations of <b>2a</b> (in situ) in varying MeOH/H <sub>2</sub> O ratios	S11
<b>Table S3.</b> Critical gel concentrations of <b>1a</b> in varying MeOH/H <sub>2</sub> O ratios	S12
<b>Figure S6.</b> Metal selectivity gelation tests	S12
<b>Figure S7.</b> Effect of added Bu <sub>4</sub> NCl on gelation	S12
<u>VI. X-ray Crystal Structures</u>	S13
<b>Figure S8.</b> Crystal structure of <b>2a</b>	S13
<b>Figure S9.</b> Solid-state packing of <b>2a</b>	S14
<b>Figure S10.</b> Crystal structure of <b>S1</b>	S14
<b>Figure S11.</b> Solid-state packing of <b>S1</b>	
<u>VII. Scanning Electron Microscope Images</u>	S15
<b>Figure S12.</b> SEM images of gel of <b>2a</b> (in situ)	S16
<b>Figure S13.</b> SEM images of gel of <b>2a</b> (complex)	S16
<b>Figure S14.</b> SEM images of gel of <b>1a</b>	

VIII. Powder X-ray Diffraction Data

<b>Figure S15.</b> PXRD patterns of <b>2a</b>	S17
<b>Figure S16.</b> PXRD patterns for gels of <b>2a</b> in situ and as isolated complex	S17
<b>Figure S17.</b> PXRD patterns for Hg(OAc) <sub>2</sub> and <b>1a</b> simulated from its crystal structure	S18

IX. Rheological Data

<b>Figure S18.</b> Frequency sweep data for a gel of <b>2a</b>	S19
<b>Figure S19.</b> Strain and oscillatory stress sweep data for a gel of <b>2a</b>	S19

X. Inductively Coupled Plasma-Optical Emission Spectroscopy Data

<b>Table S4.</b> Summary of data for mercury detection	S20
<b>Figure S20.</b> Calibration curve for ICP-OES analysis of <b>2a</b>	S20

## I. Materials

All reagent grade materials and solvents were purchased from Sigma-Aldrich, Acros, or TCI and used without further purification.

## II. General Experimental

Complex Gel Formation – An 8 mL vial was charged with **2a** (13 mg, 0.026 mmol) and a MeOH/H<sub>2</sub>O (90/10 v/v, 1 mL) solution. The vial was sealed and the mixture was heated until homogeneous and then cooled to rt to form a gel.

In Situ Gel Formation – An 8 mL vial was charged with **1a** (7 mg, 0.05 mmol) and MeOH (0.9 mL) and heated to dissolve. An aq. Hg(OAc)<sub>2</sub> solution (0.1 mL, 0.157 M) was then added. The vial was sealed and the mixture was heated until homogeneous and then cooled to rt to form a gel.

Gelation Selectivity Tests – Six 12 mL vials were charged with **1a** (10 mg, 0.068 mmol) in MeOH (0.8 mL) and heated to dissolve. One of an array of aq. solutions of metal acetate salts (AgOAc, Ba(OAc)<sub>2</sub>, Cd(OAc)<sub>2</sub>, Co(OAc)<sub>2</sub>, Cu(OAc)<sub>2</sub>, Ni(OAc)<sub>2</sub>; 0.2 mL, 0.157 M) were added to each vial. The vials were sealed, the mixtures were heated until homogeneous, and then cooled to rt. No gels were observed.

Counter Ion Effect Test – In situ gels of **2a** were prepared according to the general procedure in MeOH/H<sub>2</sub>O (90/10 v/v). Various amounts (0, 0.5, 1.0, and 2.0 equiv) of Bu<sub>4</sub>NCl was added to the stable gel. The photos were taken 10 min after adding Bu<sub>4</sub>NCl.

NMR Spectroscopy – <sup>1</sup>H and <sup>13</sup>C NMR spectra for all compounds were acquired in d<sub>6</sub>-DMSO on a Varian MR400 Spectrometer operating at 400 MHz and 100 MHz, respectively. The chemical shift data are reported in units of δ (ppm) relative to tetramethylsilane and referenced with residual DMSO.

X-ray Crystallography – Colorless plates of **2a** were crystallized from a DMSO/H<sub>2</sub>O solution at 23 °C. A crystal of dimensions 0.23 x 0.12 x 0.03 mm was mounted on a standard Bruker SMART-APEX CCD-based X-ray diffractometer equipped with a low temperature device and fine focus Mo-target X-ray tube (λ = 0.71073 Å) operated at 1500 W power (50 kV, 30 mA). The X-ray intensities were measured at 85(2) K; the detector was placed at a distance 5.055 cm from the crystal. A total of 5190 frames were collected with a scan width of 0.5° in Φ and 0.45° with an exposure time of 25 s/frame. The frames were integrated with the Bruker SAINT software package with a narrow frame algorithm. The integration of the data yielded a total of 17188 reflections to a maximum 2θ value of 59.26° of which 1952 were independent and 1952 were greater than 2σ(I). The final cell constants were based on the xyz centroids of 9871 reflections above 10σ(I). Analysis of the data showed negligible decay during data collection; the data were processed with SADABS and corrected for absorption. The structure was solved and refined with the Bruker SHELXTL (version 2008/4) software package,<sup>1</sup> using the space group P1̄bar with Z = 1 for the formula C<sub>16</sub>H<sub>10</sub>N<sub>4</sub>O<sub>2</sub>Hg. All non-hydrogen atoms were refined anisotropically with the hydrogen atoms placed in idealized positions. The complex occupies an inversion center in the crystal lattice. Full-matrix least-squares refinement based on F<sup>2</sup> converged at R<sub>1</sub> = 0.0320 and wR<sub>2</sub> = 0.0777 [based on I > 2σ(I)], R<sub>1</sub> = 0.0320 and wR<sub>2</sub> = 0.0777 for all data. Additional details are presented in Figures S8-S9 and are also given as Supporting Information in a CIF file.

Colorless plates of **S1** were crystallized from a MeOH solution at 23 °C. A crystal of dimensions 0.37 x 0.34 x 0.10 mm was mounted on a standard Bruker SMART-APEX CCD-based X-ray diffractometer equipped with a low temperature device and fine focus Mo-target X-ray tube ( $\lambda = 0.71073 \text{ \AA}$ ) operated at 1500 W power (50 kV, 30 mA). The X-ray intensities were measured at 85(2) K; the detector was placed at a distance 5.055 cm from the crystal. A total of 2085 frames were collected with a scan width of  $1.5^\circ$  in  $\Phi$  and  $\theta$  with an exposure time of 5 s/frame. The frames were integrated with the Bruker SAINT software package with a narrow frame algorithm. The integration of the data yielded a total of 18315 reflections to a maximum  $2\theta$  value of  $60.04^\circ$  of which 2315 were independent and 2308 were greater than  $2s(I)$ . The final cell constants were based on the xyz centroids of 9861 reflections above  $10s(I)$ . Analysis of the data showed negligible decay during data collection; the data were processed with SADABS and corrected for absorption. The structure was solved and refined with the Bruker SHELXTL (version 2008/4) software package,<sup>1</sup> using the space group P1bar with  $Z = 1$  for the formula  $C_{16}H_{12}N_4O_2HgCl_2$ . All non-hydrogen atoms were refined anisotropically with the hydrogen atoms placed in idealized positions. The complex occupies an inversion center in the crystal lattice. Full-matrix least-squares refinement based on  $F^2$  converged at  $R1 = 0.0596$  and  $wR2 = 0.1670$  [based on  $I > 2\sigma(I)$ ],  $R1 = 0.0600$  and  $wR2 = 0.1677$  for all data. Additional details are presented in Figures S10-S11 and are given as Supporting Information in a CIF file.

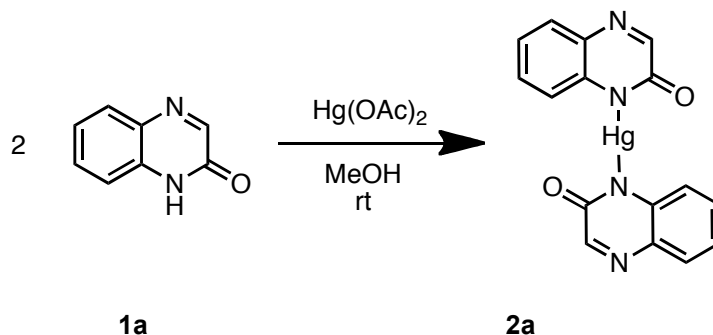
Powder X-ray Diffraction – Powder X-ray diffraction (PXRD) patterns were collected at ambient temperature using a Bruker D8 Advance diffractometer with a LynxEye detector using graphite monochromated Cu-K $\alpha$  radiation (1.5406 Å). The samples were loaded onto glass microscope slides. The software used for data analysis was JADE.

Scanning Electron Microscopy (SEM) – Gels were prepared according to the general procedure. Wet gels were placed in an SEM holder mounted onto SEM stubs with copper tape, and observed using the low vacuum mode of a Philips XL30FEG SEM and a 15-kV accelerating voltage. The images were digitally recorded and processed using Adobe Illustrator.

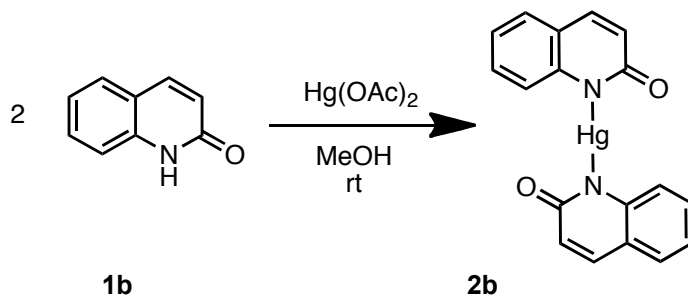
Rheology – Rheological measurements were taken on an AR2000ex rheometer (TA Instruments) with a 25 mm parallel plate. The gap was fixed at 300  $\mu\text{m}$ . A gel sample was pre-formed in a 4 mL vial and transferred onto the Peltier plate. To prevent solvent evaporation, the loaded sample was covered with a solvent trap. All measurements were performed at 25 °C. The frequency sweep study was performed under 0.2 Pa stress with a frequency range from 0.628 rad/s to 628 rad/s (i.e., 0.1 Hz – 100 Hz). The strain sweep study was performed with a strain ramp from 0.0174% to 10% at a frequency of 1 Hz. The oscillation stress sweep was performed at 1 Hz, with a stress ranging from 0.008 Pa to 100 Pa.

Inductively Coupled Plasma-Optical Emission Spectroscopy – Inductively coupled plasma-optical emission spectroscopy (ICP-OES) measurements were taken on a Perkin-Elmer Optima 2000 DV. The detection limit for mercury was approximately 10 ppb. Mercury was analyzed with a wavelength of 253.652 nm. Yttrium was used as an internal standard and detected with a wavelength of 371.029 nm. A calibration curve was generated by preparing 4 standard solutions (1 ppm Y; 0, 1, 5, 10 ppm Hg, Figure S19). Three measurements were taken for each sample and averaged.

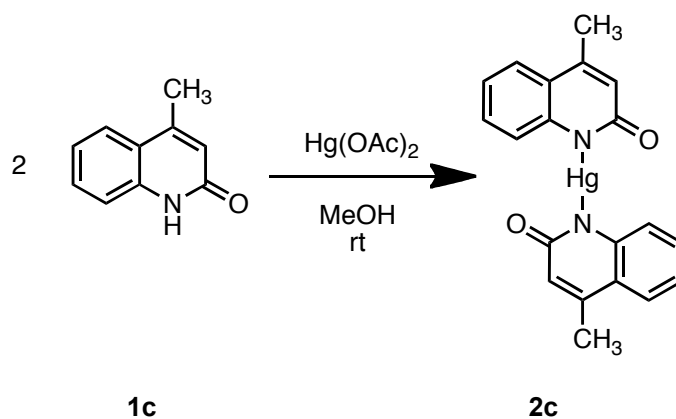
### III. Synthetic Procedures<sup>2</sup>



**2a:** **1a** (46 mg, 0.31 mmol) was dissolved in MeOH (20 mL). Then  $\text{Hg}(\text{OAc})_2$  (50 mg, 0.16 mmol) was dissolved in MeOH (5 mL) and added to produce an off-white precipitate (**2a**). The precipitate was filtered and washed with  $\text{H}_2\text{O}$  (1 x 20 mL). **2a** was purified by recrystallization from MeOH to give 67 mg (86% yield) of a light brown solid. HRMS (ESI): Calcd for  $\text{C}_{16}\text{H}_{10}\text{N}_4\text{O}_2\text{Hg}$ , 492.0510; found, 492.0522. Elemental analysis: Calcd for  $\text{C}_{16}\text{H}_{10}\text{N}_4\text{O}_2\text{Hg}$ : C, 39.15%; H, 2.05%; N, 11.41%; found: C, 39.21%; H, 2.05%; N, 11.53%.

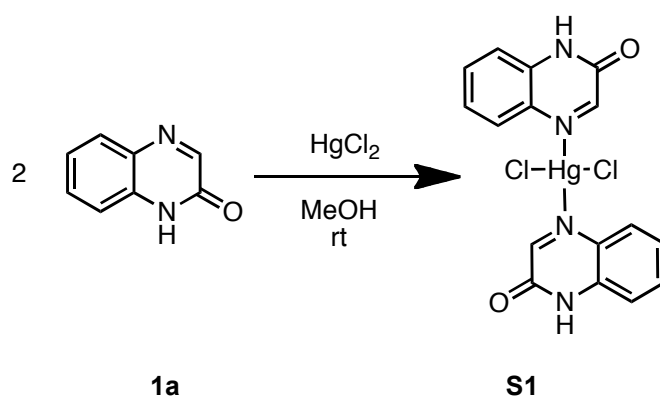


**2b:** **1b** (46 mg, 0.31 mmol) was dissolved in MeOH (20 mL). Then  $\text{Hg}(\text{OAc})_2$  (50 mg, 0.16 mmol) was dissolved in MeOH (5 mL) and added to produce an off-white precipitate (**2b**). The precipitate was filtered and washed with  $\text{H}_2\text{O}$  (1 x 20 mL). **2b** was purified by recrystallization from MeOH to give 64 mg (82% yield) of a white solid. HRMS (ESI): Calcd. For  $\text{C}_{18}\text{H}_{12}\text{N}_2\text{O}_2\text{Hg}$ , 490.0605; found, 490.0617.



**2c:** **1c** (50 mg, 0.31 mmol) was dissolved in MeOH (20 mL). Then Hg(OAc)<sub>2</sub> (50 mg, 0.16 mmol) was dissolved in MeOH (5 mL) and added to produce an off-white precipitate (**2c**). The precipitate was filtered and washed with H<sub>2</sub>O (1 x 20 mL). **2c** was purified by recrystallization from MeOH to give 73 mg (88% yield) of a white solid. HRMS (ESI): Calcd. For C<sub>20</sub>H<sub>16</sub>N<sub>2</sub>O<sub>2</sub>Hg, 518.0918; found, 518.0923.

---



**S1:** **1a** (46 mg, 0.31 mmol) was dissolved in MeOH (20 mL). Then HgCl<sub>2</sub> (50 mg, 0.18 mmol) was dissolved in MeOH (5 mL) and added to produce light brown crystals (**S1**). The precipitate was filtered and washed with H<sub>2</sub>O (1 x 20 mL). **S1** was purified by recrystallization from MeOH to give 49 mg (48% yield) of a light brown solid.

#### IV. NMR Spectra

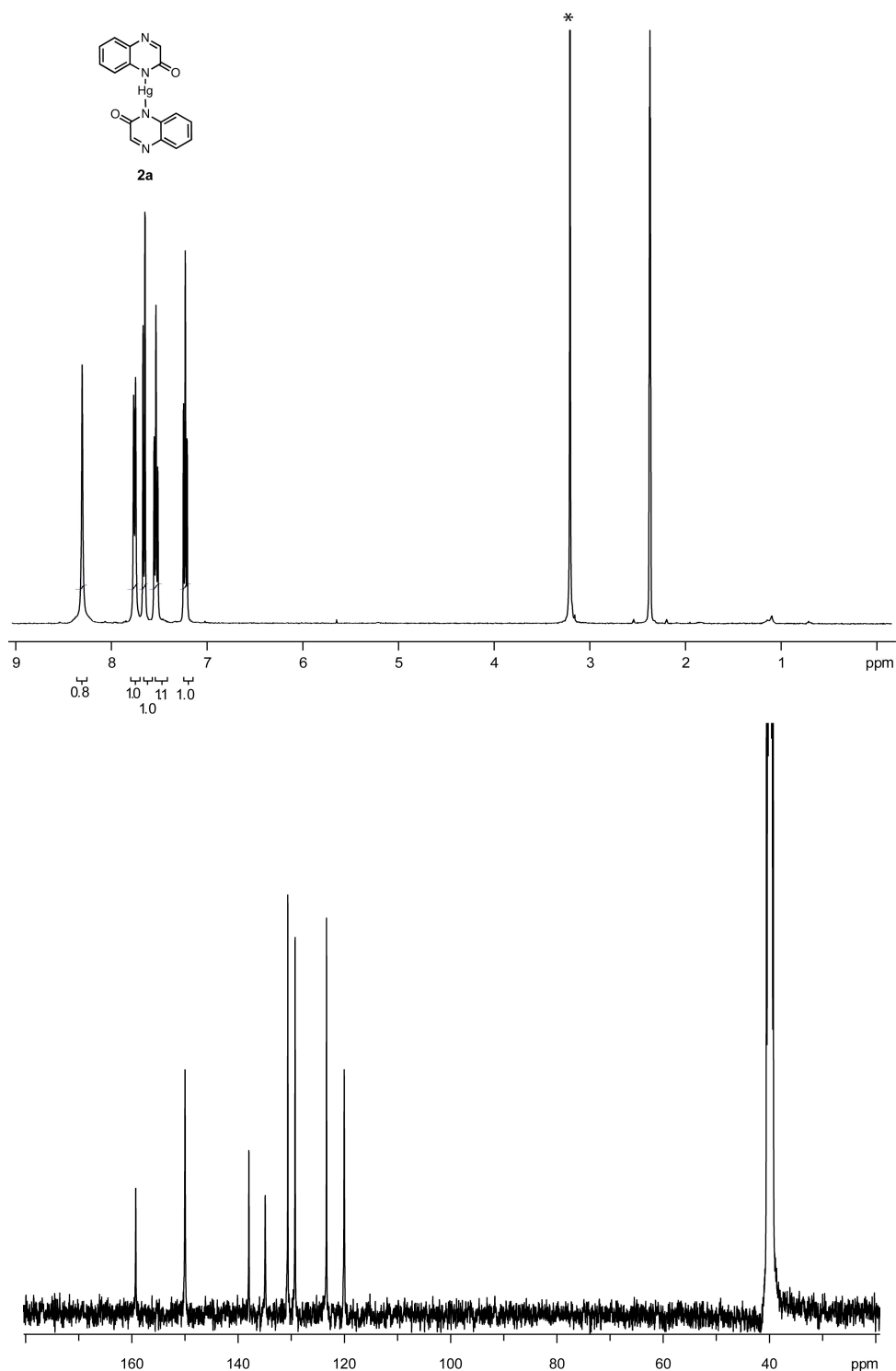


**Figure S1.**  $^1\text{H}$  and  $^{13}\text{C}$  NMR spectra of **2a**.  $^1\text{H}$  NMR (400 MHz,  $d_6$ -DMSO)  $\delta$  8.40 (s, 1H), 7.80 (d,  $J = 7.8$  Hz, 1H), 7.70 (d,  $J = 7.8$  Hz, 1H), 7.58 (dt,  $J = 1.2, 7.0$  Hz, 1H), 7.27 (dt,  $J = 1.2, 7.0$  Hz, 1H).  $^{13}\text{C}$  NMR (100 MHz,  $d_6$ -DMSO)  $\delta$  159.26, 149.98, 137.96, 134.89, 130.64, 129.27, 123.35, 120.02. \*denotes residual  $\text{H}_2\text{O}$  in  $d_6$ -DMSO.

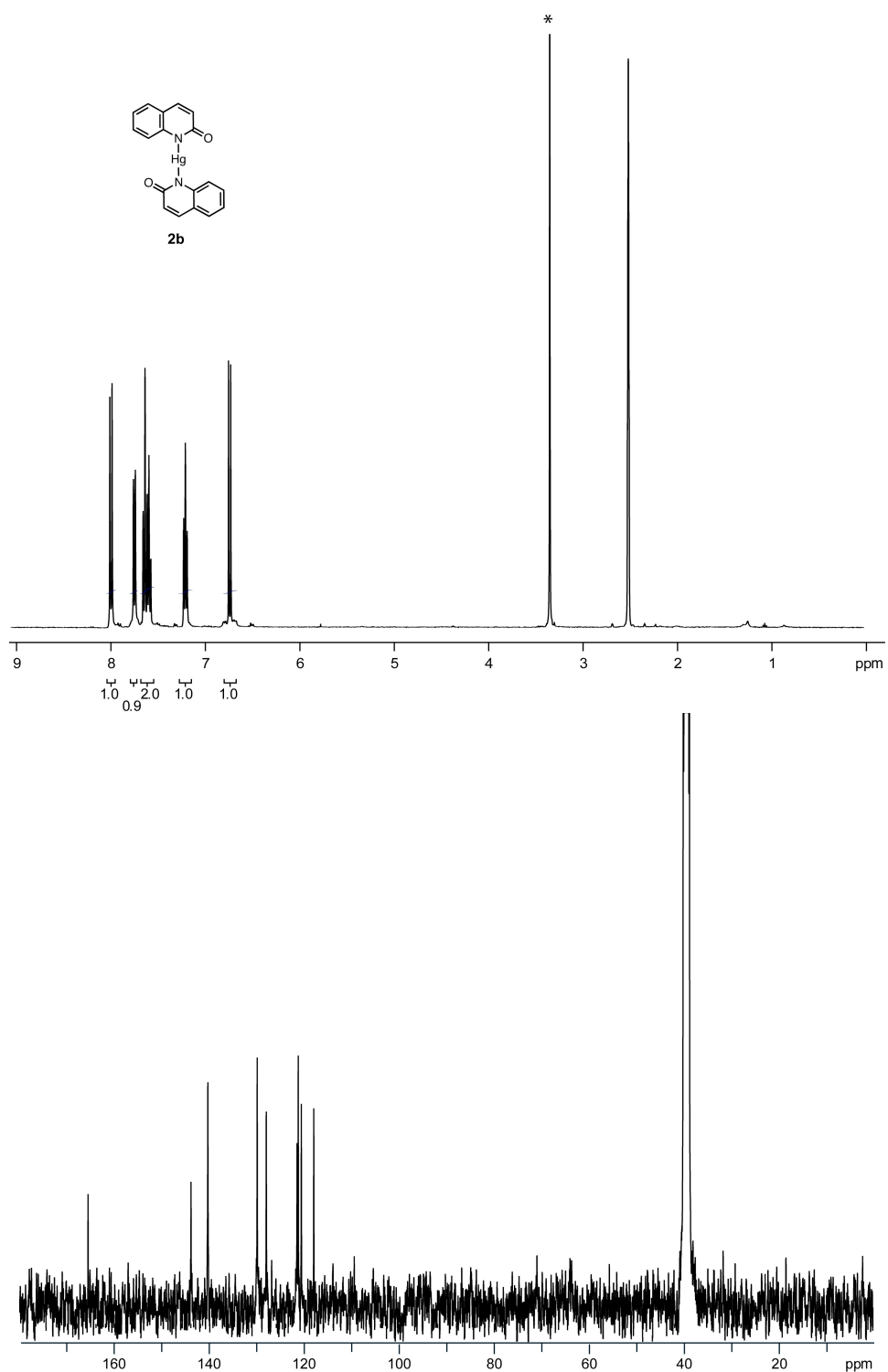


**Figure S2.**  $^1\text{H}$  and  $^{13}\text{C}$  NMR spectra of **2b**.  $^1\text{H}$  NMR (400 MHz,  $d_6$ -DMSO)  $\delta$  7.92 (d,  $J$  = 9.2 Hz, 1H), 7.67 (d,  $J$  = 7.8 Hz, 1H), 7.54 (m, 2H), 7.13 (dt,  $J$  = 1.2, 6.6 Hz, 1H), 6.66 (d,  $J$  = 9.2 Hz, 1H).  $^{13}\text{C}$  NMR (100 MHz,  $d_6$ -DMSO)  $\delta$  166.07, 144.36, 140.81, 130.40, 128.49, 122.00, 121.75, 121.10, 118.47. \*denotes residual  $\text{H}_2\text{O}$  in  $d_6$ -DMSO.

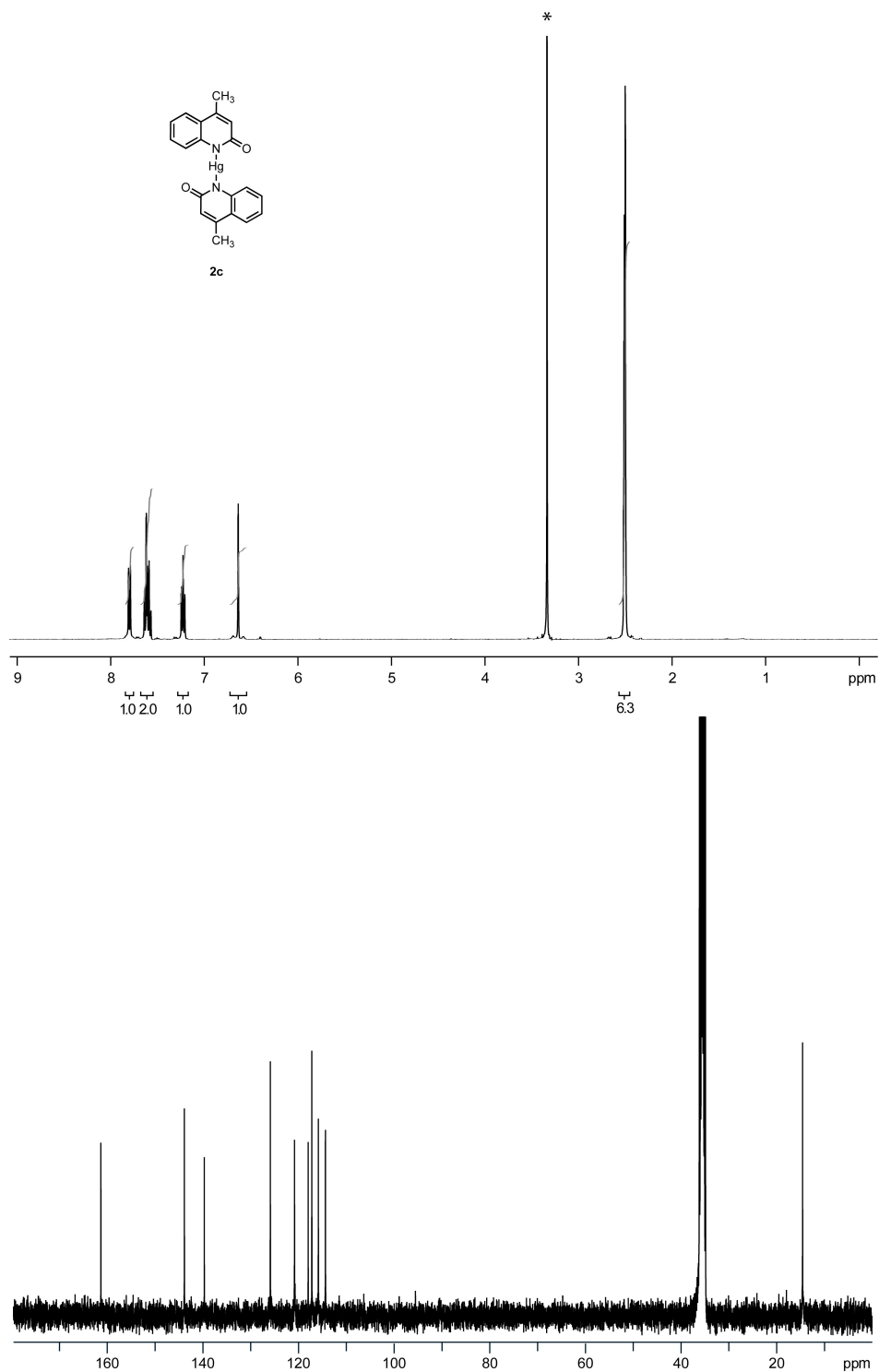


**Figure S3.** <sup>1</sup>H and <sup>13</sup>C NMR spectra of **2c**. <sup>1</sup>H NMR (400 MHz, *d*<sub>6</sub>-DMSO) δ 7.79 (d, *J* = 8.0 Hz, 1H), 7.62 (m, 2H), 7.23 (dt, *J* = 1.5, 5.3 Hz, 1H), 6.64 (d, *J* = 1.0 Hz, 1H), 2.51 (3H, overlap with solvent peak). <sup>13</sup>C NMR (100 MHz, *d*<sub>6</sub>-DMSO) δ 161.32, 143.86, 139.69, 125.88, 120.82, 117.97, 117.21, 115.84, 114.36, 14.56. \*denotes residual H<sub>2</sub>O in *d*<sub>6</sub>-DMSO.

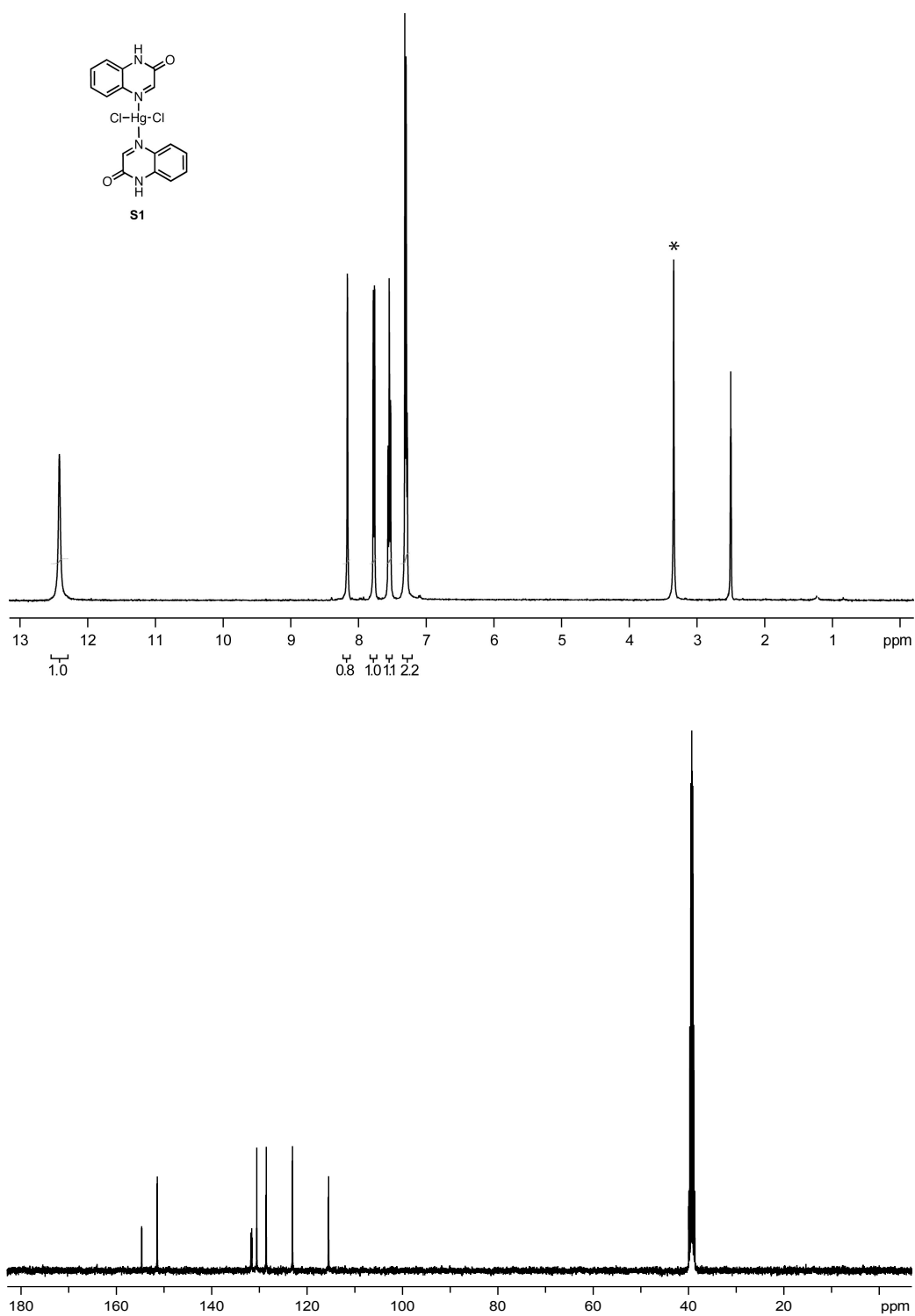


**Figure S4.** <sup>1</sup>H and <sup>13</sup>C NMR spectra of **S1**. <sup>1</sup>H NMR (400 MHz, *d*<sub>6</sub>-DMSO) δ 12.38 (s, 1H), 8.16 (s, 1H), 7.77 (dd, *J* = 1.1, 7.4 Hz, 1H), 7.53 (dt, *J* = 1.1, 6.7 Hz, 1H), 7.30 (t, *J* = 7.4 Hz, 2H). <sup>13</sup>C NMR (100 MHz, *d*<sub>6</sub>-DMSO) δ 154.67, 151.42, 131.79, 131.59, 130.54, 128.56, 123.04, 115.48. \*denotes residual H<sub>2</sub>O in *d*<sub>6</sub>-DMSO.

## V. Gelation Tests

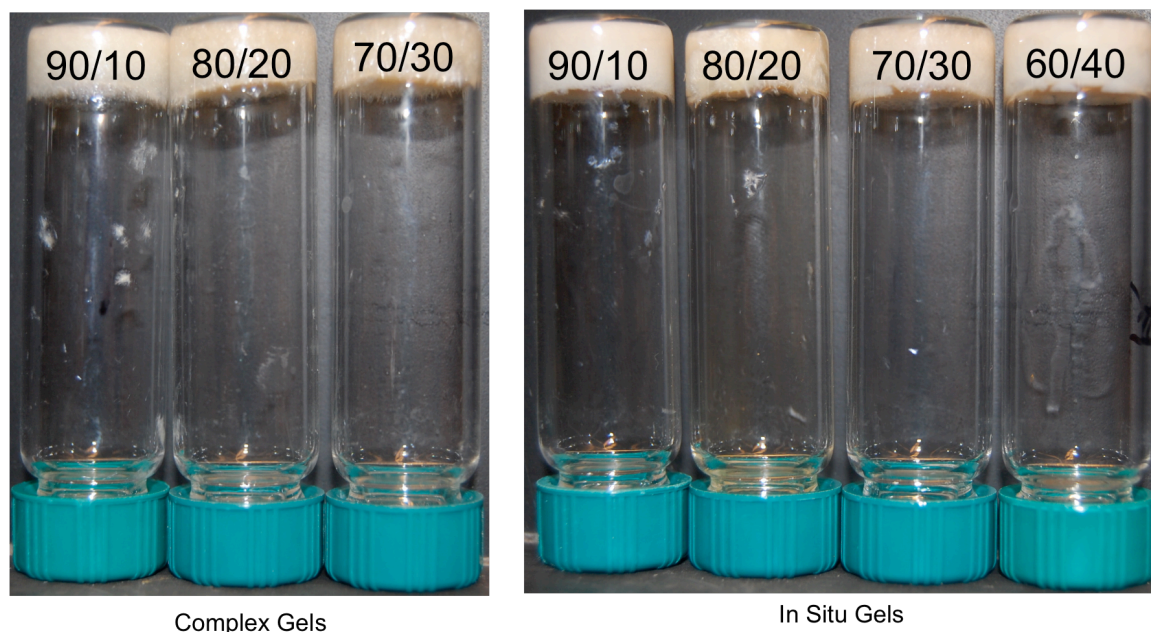


**Figure S5.** Gels of **2a** at their respective critical gel concentrations (cgc) in 1 mL of varying MeOH/H<sub>2</sub>O ratios (see Tables S1 and S2).

**Table S1.** Cgcs of **2a** (complex) in 1 mL of varying MeOH/H<sub>2</sub>O ratios at 25 °C.

MeOH/H <sub>2</sub> O (v/v)	Trial 1 (mM)	Trial 2 (mM)	Trial 3 (mM)	average cgc (mM)	wt % (average)
90/10	24	26	26	25 ± 1	1.6
80/20	24	22	26	24 ± 2	1.5
70/30	26	26	26	26 ± 0	1.6

**Table S2.** Cgcs of **2a** (in situ) in 1 mL of varying MeOH/H<sub>2</sub>O ratios at 25 °C. The molarities were calculated assuming quantitative formation of **2a**.

MeOH/H <sub>2</sub> O (v/v)	Trial 1 (mM)	Trial 2 (mM)	Trial 3 (mM)	average cgc (mM)	wt % (average)
90/10	24	21	24	23 ± 2	1.2
80/20	24	24	24	24 ± 0	1.3
70/30	21	21	24	22 ± 2	1.2
60/40	21	21	21	21 ± 0	1.1

**Table S3.** Cgcs of **1a** in 1 mL of varying MeOH/H<sub>2</sub>O ratios at 25 °C

MeOH/H <sub>2</sub> O (v/v)	Trial 1 (mM)	Trial 2 (mM)	Trial 3 (mM)	average cgc (mM)	wt % (average)
90/10	191	185	198	191 ± 6	3.4
80/20	164	164	157	162 ± 4	2.5
70/30	150	157	157	155 ± 4	2.4



**Figure S6.** Selectivity tests showing the results of adding aq. solutions of an array of metal acetate salts (0.2 mL, 0.157 M) to a solution of **1a** (10 mg, 0.068 mmol) in MeOH (0.8 mL). Metal salts from left to right: Hg(OAc)<sub>2</sub>, Ba(OAc)<sub>2</sub>, Cd(OAc)<sub>2</sub>, Cu(OAc)<sub>2</sub>, Co(OAc)<sub>2</sub>, Ni(OAc)<sub>2</sub>, AgOAc. The only gel that formed was with Hg(OAc)<sub>2</sub>.



**Figure S7.** The effect of adding Bu<sub>4</sub>NCl to a gel of **2a** (in situ) above cgc (20 mg/mL). The images show the gel sample 10 min after adding (from left to right) 0, 0.5, 1.0, and 2.0 equiv of Bu<sub>4</sub>NCl.

## VI. X-ray Crystal Structures

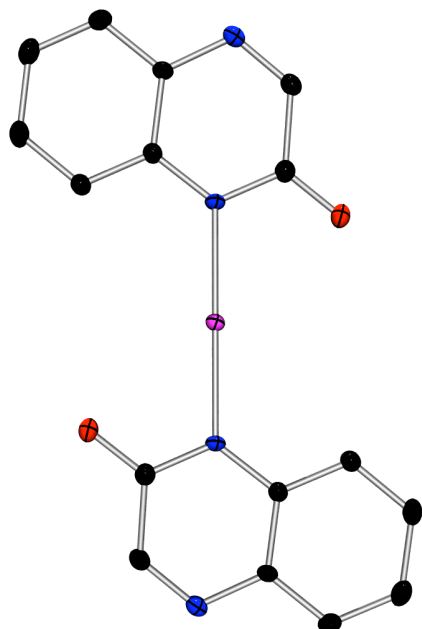


**Figure S8.** Crystal structure of **2a**. The torsion angle between the quinoxalinone ligands is  $4.41^\circ$ . The Hg-N bond length is  $2.04 \text{ \AA}$  and the N-Hg-N bond angle is  $180.00^\circ$ . The hydrogen atoms were omitted for clarity.

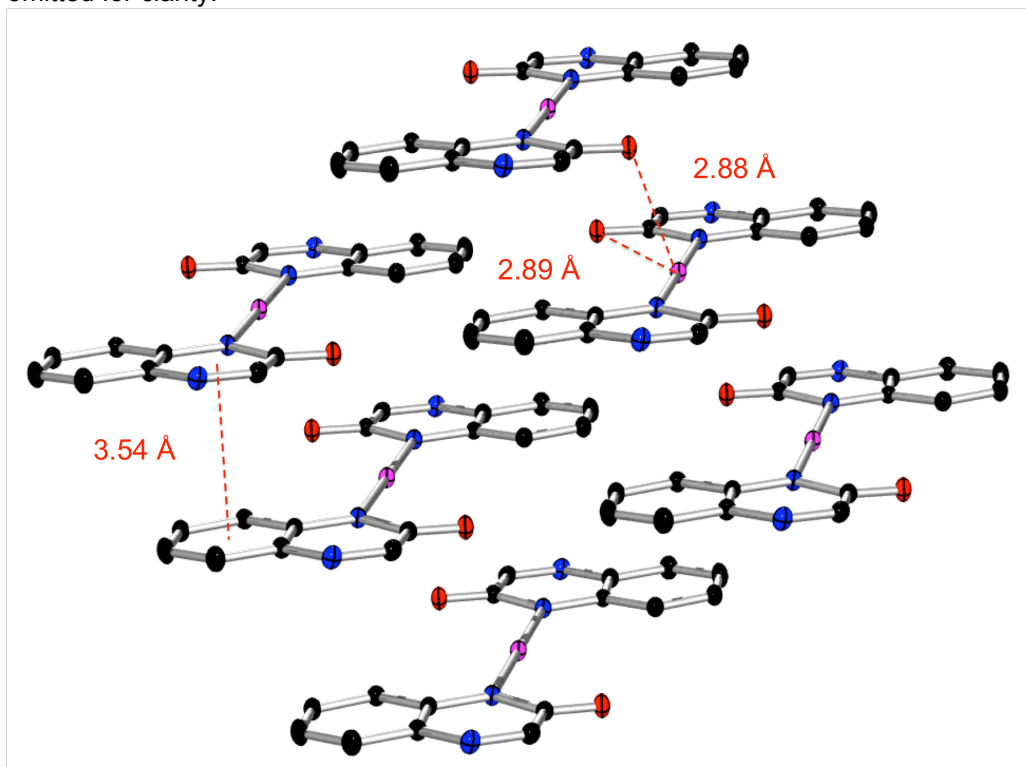


**Figure S9.** Solid-state packing of **2a**. The aryl-aryl  $\pi$ -stacking distance is  $3.54 \text{ \AA}$ . The intramolecular Hg-O distance is  $2.89 \text{ \AA}$  while the intermolecular Hg-O distance is  $2.88 \text{ \AA}$ . The hydrogen atoms were omitted for clarity.

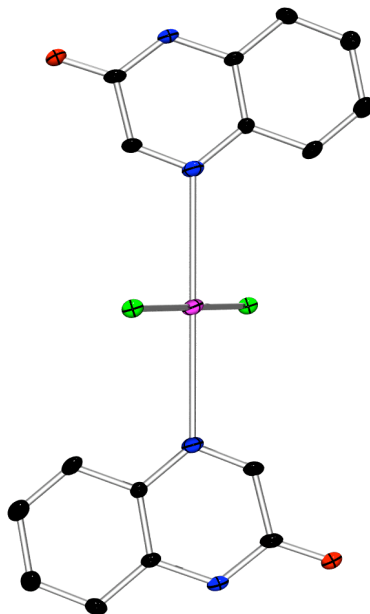


**Figure S10.** Crystal structure of **S1**. The torsion angle between the quinoxalinone ligands is  $14.47^\circ$ . The Hg-N bond length is  $2.74 \text{ \AA}$  and the N-Hg-N bond angle is  $180.00^\circ$ . The hydrogen atoms were omitted for clarity.

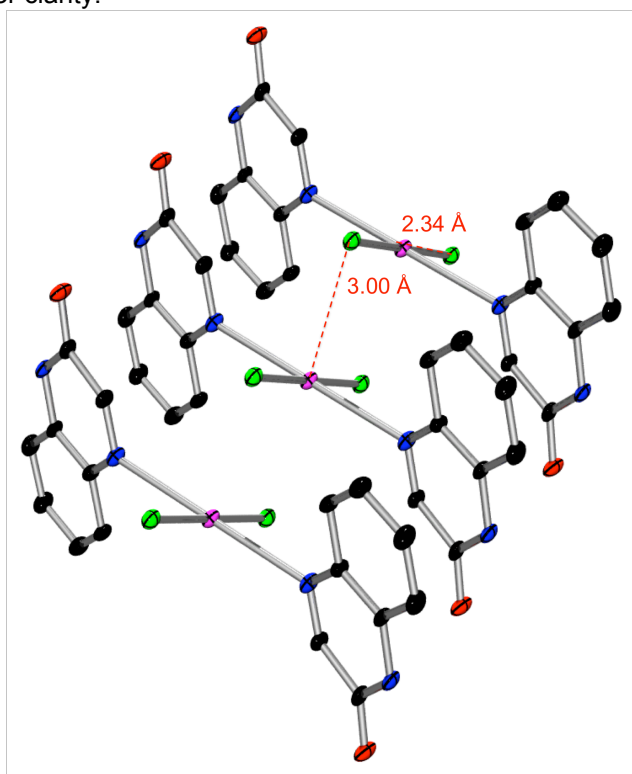


**Figure S11.** Solid-state packing of **S1**. The Hg-Cl bond length is  $2.34 \text{ \AA}$  and the intermolecular distance between Hg-Cl atoms is  $3.00 \text{ \AA}$ . The distance between offset aryl rings is  $3.78 \text{ \AA}$ . The hydrogen atoms were omitted for clarity.

## VII. SEM Images

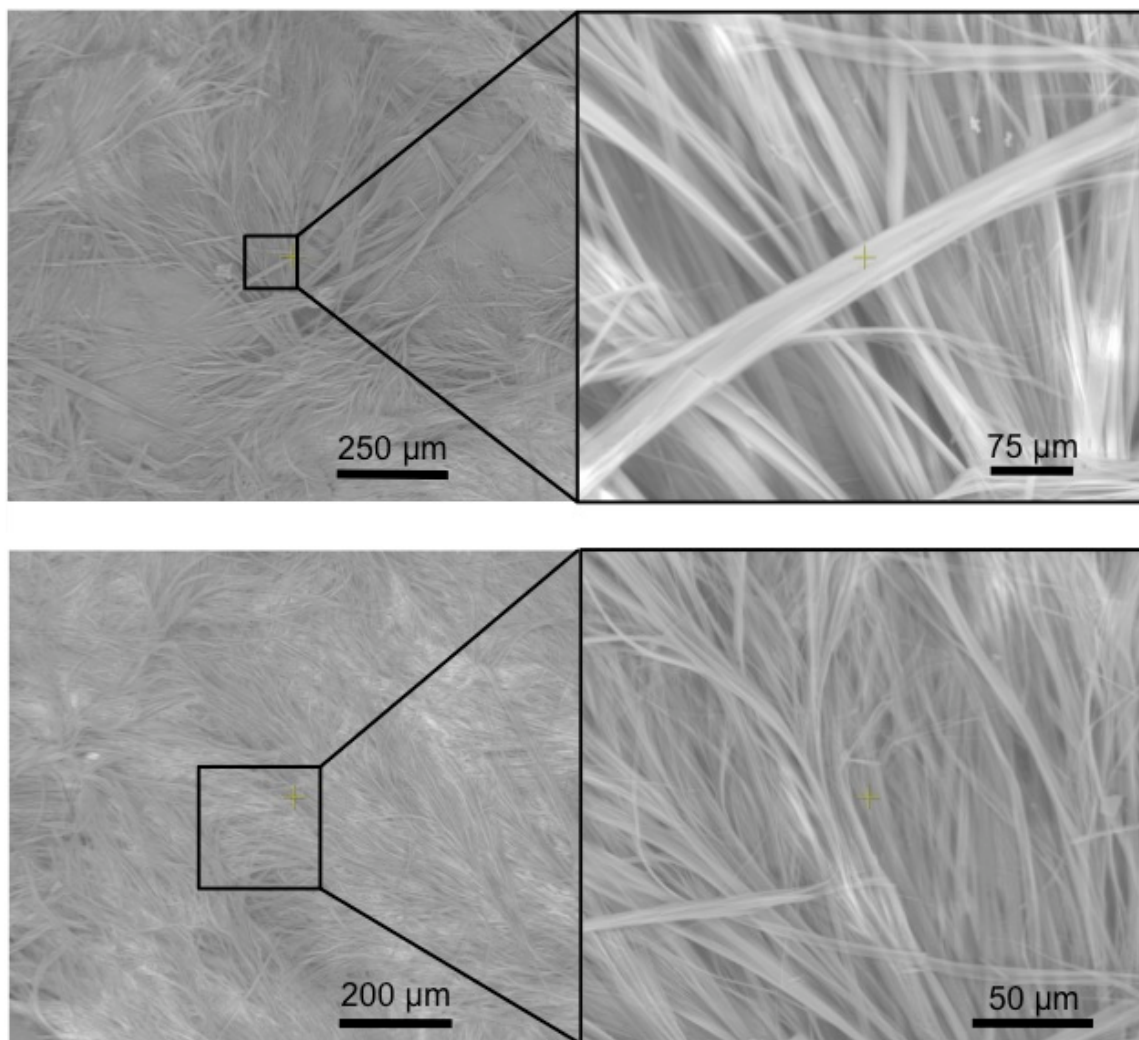


**Figure S12.** SEM images of an in situ gel of **2a** (24 mM) in 90/10 MeOH/H<sub>2</sub>O. The images on the right are at a higher magnification.

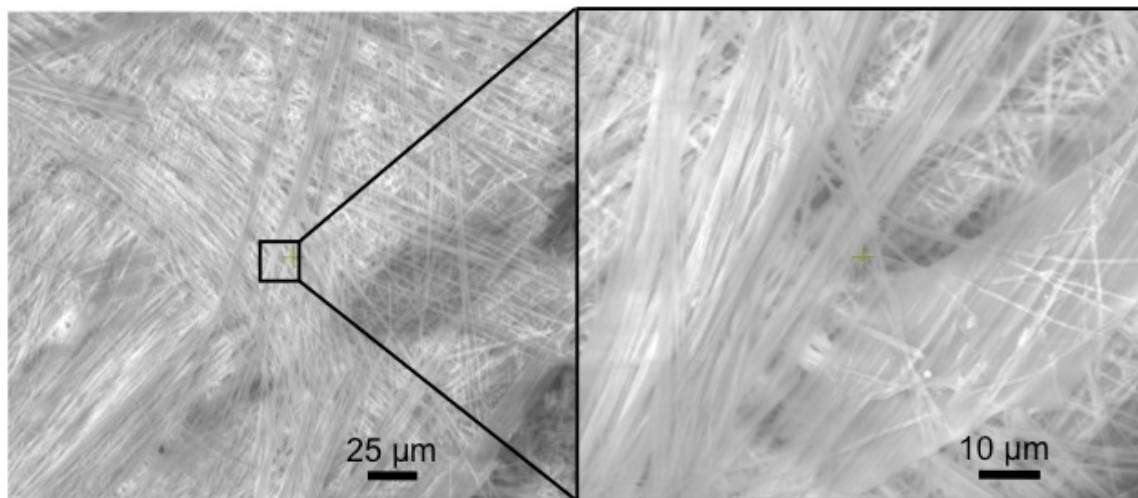


**Figure S13.** SEM image of a gel of **2a** (complex) (25 mM) in 90/10 MeOH/H<sub>2</sub>O. The image on the right is at a higher magnification.

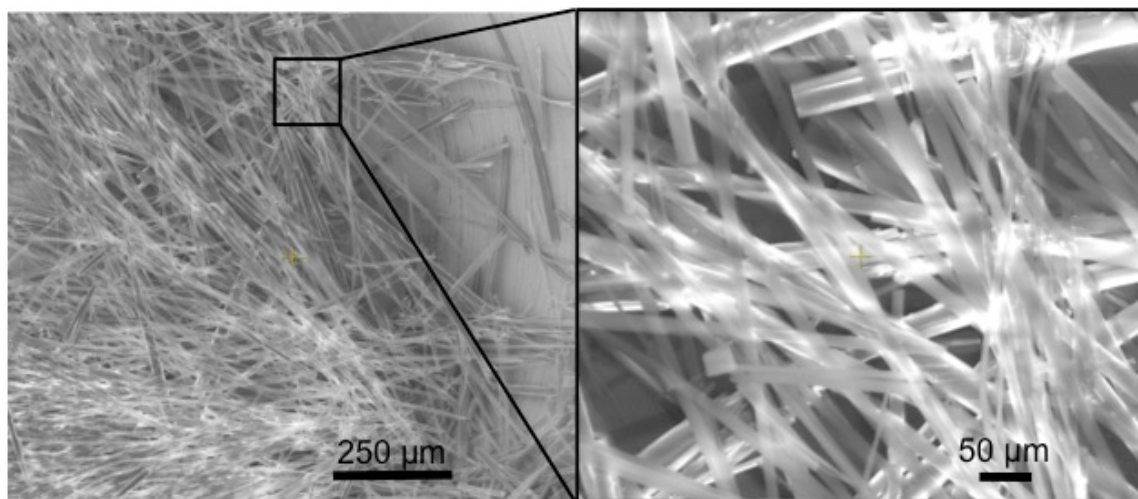


**Figure S14.** SEM image of **1a** (191 mM) in 70/30 MeOH/H<sub>2</sub>O. The image on the right is at a higher magnification.

### VIII. Powder X-ray Diffraction Data

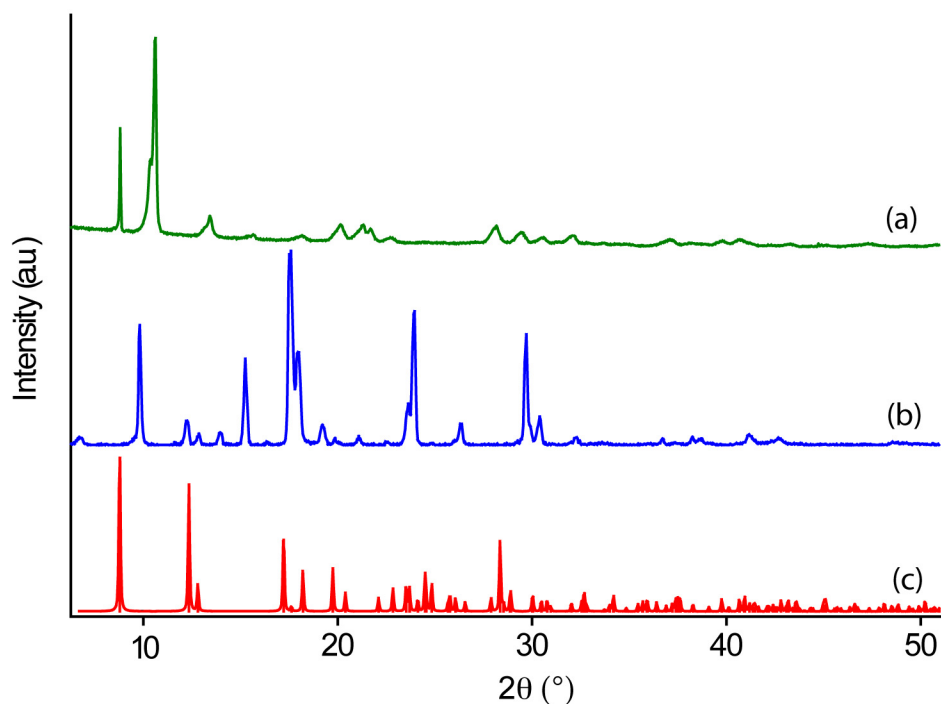


**Figure S15.** Powder X-ray diffraction patterns of (a) **2a** precipitated from MeOH, (b) a gel of **2a** (from isolated complex, 90/10 MeOH/H<sub>2</sub>O), and (c) simulated from the crystal structure of **2a**.

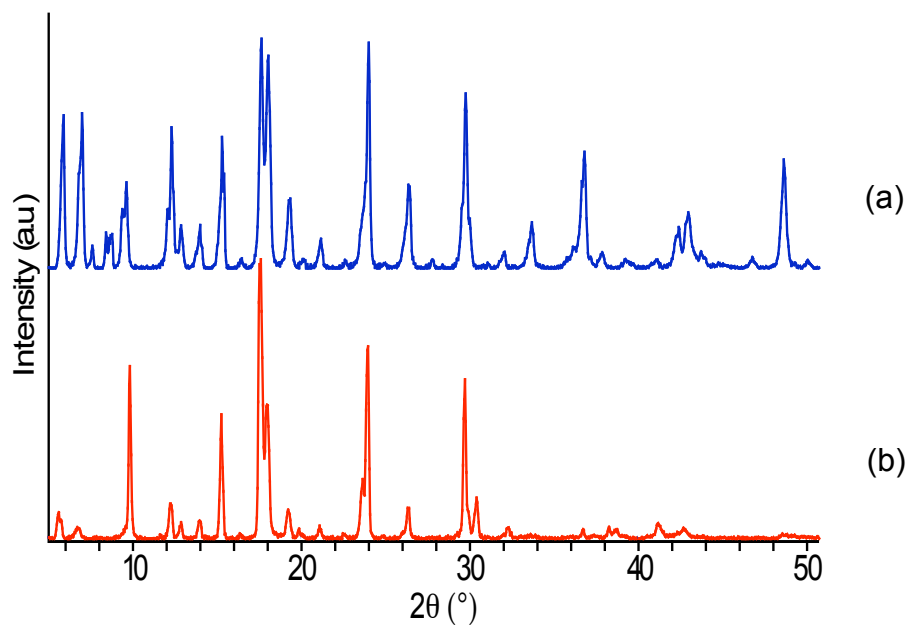


**Figure S16.** Powder X-ray diffraction patterns for gels of (a) **2a** (in situ) and (b) **2a** (isolated complex).

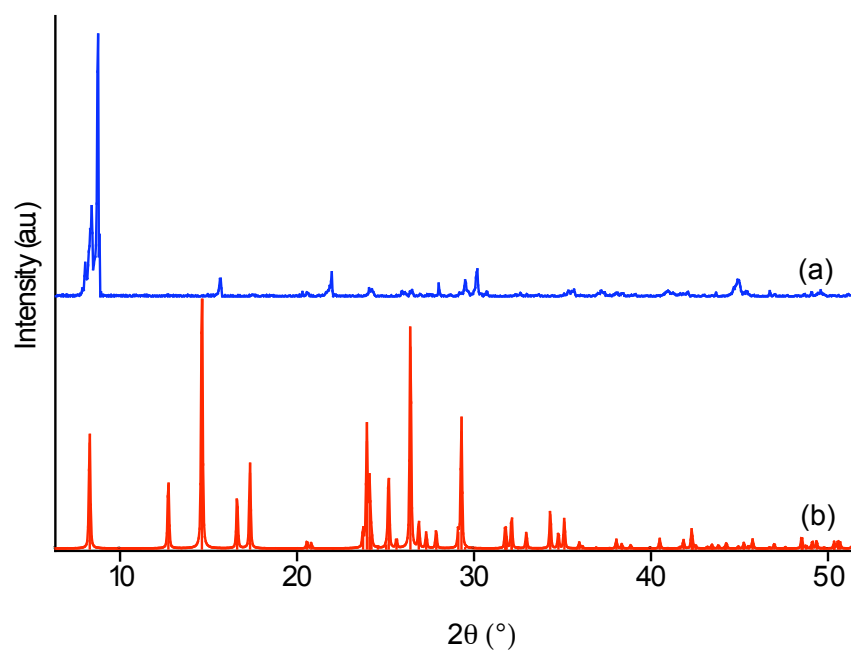


**Figure S17.** Powder X-ray diffraction patterns for (a) Hg(OAc)<sub>2</sub> and (b) **1a** simulated from the crystal structure.

## IX. Rheological Data

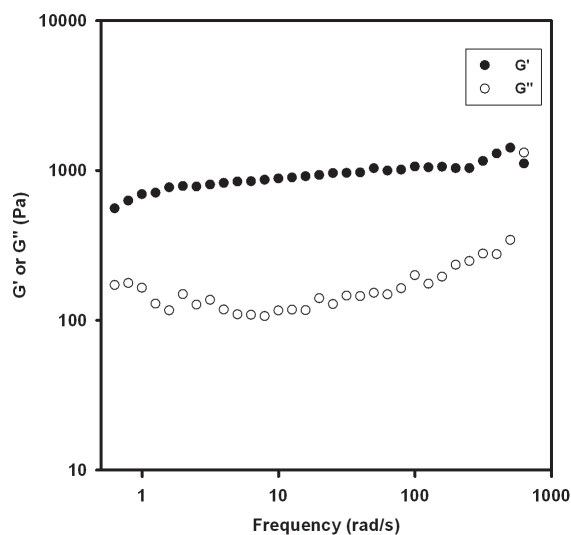


**Figure S18.** Frequency sweep data under a constant stress (0.2 Pa) for a gel of **2a** (20 mg/mL) in MeOH/H<sub>2</sub>O (90/10 v/v). The samples are viscoelastic, with the storage modulus ( $G'$ ) 5 times larger than loss modulus ( $G''$ ).

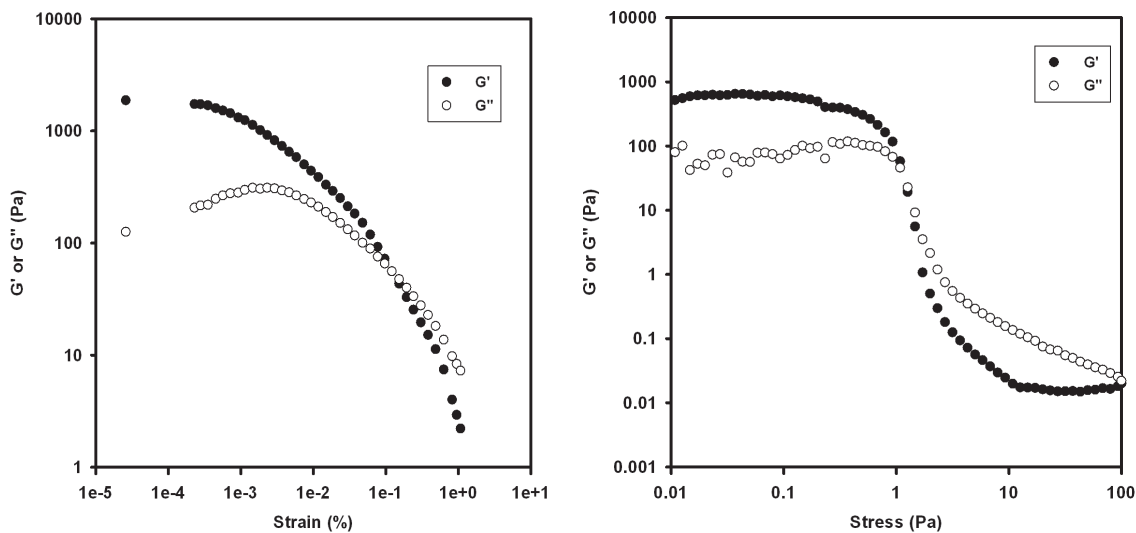


**Figure S19. Left:** Strain sweep data for a gel of **2a** (20 mg/mL, 90/10 MeOH/H<sub>2</sub>O) acquired under constant frequency (1 Hz). The gel network completely breaks down above strain of 0.1%. **Right:** Oscillatory stress sweep measurements for a gel of **2a** (20 mg/mL, 90/10 MeOH/H<sub>2</sub>O) under constant frequency (1 Hz). The gel network completely breaks down at a stress of 3.7 Pa.

## X. ICP-OES Data

Representitive Procedure for ICP Samples. The samples were prepared by extraction of the syneresis (30  $\mu$ L) from an in situ **2a** gel by micropipet and diluted with H<sub>2</sub>O (to 1 mL). Residual MeOH was evaporated off using a rotary evaporator and the remaining solution was filtered using a syringe filter. The yttrium internal standard was added and samples were diluted further to 10 mL total volume with H<sub>2</sub>O. Each sample was injected three times and the average response was used to determine [Hg] with the calibration curve.

**Table 4.** ICP-OES data of the mercury concentration remaining after gelation. The table displays (from left to right) the initial mass of **1a**, the initial mass of Hg(OAc)<sub>2</sub>, the initial Hg<sup>2+</sup> concentration ([Hg]<sub>0</sub>), the concentration of Hg<sup>2+</sup> detected after gelation and sample dilution ([Hg]<sub>d</sub>), and the corresponding concentration of Hg<sup>2+</sup> in the gel ([Hg]<sub>a</sub>).

Sample	<b>1a</b> (mg)	Hg(OAc) <sub>2</sub> (mg)	[Hg] <sub>0</sub> (ppm)	[Hg] <sub>d</sub> (ppm)	[Hg] <sub>a</sub> (ppm)
1	7	7	4400	1.07 ± 0.02	358
2	7	8	5000	1.86 ± 0.01	621
3	7	6	3800	0.867 ± 0.006	289
4	7	6	3800	0.992 ± 0.005	331

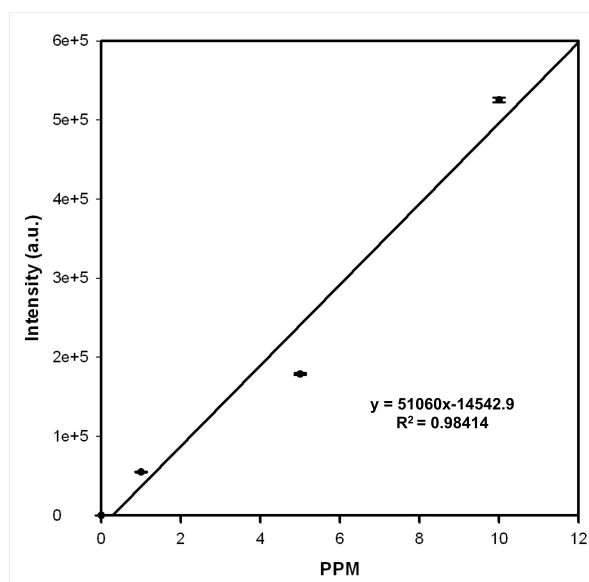


**Figure S20.** Calibration curve for ICP-OES detection of Hg<sup>2+</sup>.

## References

---

- (1) Software for X-ray Crystallography: (a) Sheldrick, G.M. SHELXTL, v. 2008/4; Bruker Analytical X-ray, Madison, WI, 2008. (b) Sheldrick, G.M. SADABS, v. 2008/1. Program for Empirical Absorption Correction of Area Detector Data, University of Gottingen: Gottingen, Germany, 2008. (c) Saint Plus, v. 7.34, Bruker Analytical X-ray, Madison, WI, 2006.
- (2) D. M. L. Goodgame, S. P. W. Hill, and D. J. Williams, *Polyhedron*, 1992, **11**, 1507-1512.